Nanocarbon Materials

DOI: 10.1002/ange.201007065

# Carbon Nanotube Wiring of Donor–Acceptor Nanograins by Self-Assembly and Efficient Charge Transport**

*Tomokazu Umeyama, Noriyasu Tezuka, Fumiaki Kawashima, Shu Seki,* Yoshihiro Matano, Yoshihide Nakao, Tetsuya Shishido, Masayuki Nishi, Kazuyuki Hirao, Heli Lehtivuori, Nikolai V. Tkachenko,* Helge Lemmetyinen, and Hiroshi Imahori**

Organic π-conjugated compounds have drawn much attention owing to their potential applications in organic thin-film optoelectronics.[1] Over the last 20 years, tremendous progress has been achieved in the design and fabrication of these compounds. In this regard, charge-transporting properties of organic thin films have found to be crucial in the device performances. It is well-known that charge transport is limited by grain boundaries in the films as well as molecular arrangements within the grains. Therefore, a new method that enhances electrical communication between the grains as well as modulating the arrangements within the grains is necessary to improve device performances.

[*] Dr. T. Umeyama, N. Tezuka, F. Kawashima, Prof. Dr. Y. Matano, Dr. Y. Nakao, Prof. Dr. T. Shishido, Prof. Dr. H. Imahori
Department of Molecular Engineering
Graduate School of Engineering, Kyoto University
Nishikyo-ku, Kyoto 615-8510 (Japan)
Fax: (+81) 75-383-2571
E-mail: imahori@scl.kyoto-u.ac.jp

Dr. T. Umeyama, Prof. Dr. S. Seki
PRESTO (Japan) Science and Technology Agency
4-1-8 Honcho, Kawaguchi, Saitama 332-0012 (Japan)

Prof. Dr. S. Seki
Department of Applied Chemistry
Graduate School of Engineering, Osaka University
2-1, Yamadaoka, Suita, Osaka 565-0871 (Japan)

Dr. M. Nishi, Prof. Dr. K. Hirao
Department of Material Chemistry
Graduate School of Engineering, Kyoto University
Nishikyo-ku, Kyoto 615-8510 (Japan)

Dr. H. Lehtivuori, Prof. Dr. N. V. Tkachenko, Prof. Dr. H. Lemmetyinen
Department of Chemistry and Bioengineering
Tampere University of Technology
P.O. Box 541, 33101 Tampere (Finland)

Prof. Dr. H. Imahori
Institute for Integrated Cell-Material Sciences (iCeMS)
Kyoto University, Nishikyo-ku, Kyoto 615-8510 (Japan)

Prof. Dr. H. Imahori
Fukui Institute for Fundamental Chemistry, Kyoto University
Sakyo-ku, Kyoto 606-8103 (Japan)

[**] H.I. and H. Lemmetyinen thank the strategic international cooperative program with Finland (JST). T.U. is grateful for a Grant-in-Aid from Specific Area Research, MEXT (Japan) (Carbon Nanotube Nano-Electronics), the Murata Science Foundation, and the Noguchi Institute. N.T. thanks the JSPS fellowship for young scientists. H.L., N.V.T., and H.L. thank Academy of Finland.

Supporting information for this article is available on the WWW under http://dx.doi.org/10.1002/anie.201007065.

We have explored a novel self-assembly strategy to build up well-ordered donor–acceptor (D–A) nanograins and their efficient molecular wiring that can be detected as photocurrent (Figure 1). A covalent linkage between porphyrin as a donor and $C_{60}$ as an acceptor was chosen because this combination is known to yield a long-lived charge-separated

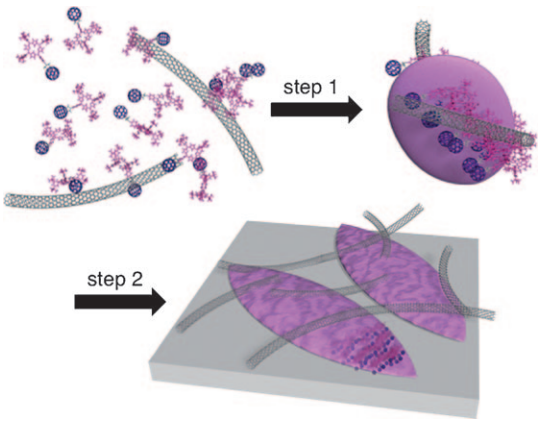


***Figure 1.*** Representation of self-assembly processes of donor–acceptor linked molecules with SWNTs onto an electrode. Step 1: rapid injection of a poor solvent, step 2: electrophoretic deposition.

state efficiently.[2] We expected that the intermolecular porphyrin–porphyrin and $C_{60}$–$C_{60}$ interactions rather than the intermolecular porphyrin–$C_{60}$ interaction would prevail to form nanograins, where D and A molecules are arranged separately for efficient photocurrent generation.[2a,3] Utilization of a semiflexible, short methylene spacer between the porphyrin and $C_{60}$ would be suitable to strengthen the desirable interactions. Rapid injection of a poor solvent into a good solvent containing the D–A linked dyads was used to accelerate the formation of D–A nanograins in the mixed solvent (step 1 in Figure 1).[2b] More importantly, an addition of single-walled carbon nanotubes (SWNTs) as a molecular wire was anticipated to cross-link the D–A nanograins in the mixed solvent simultaneously (step 1 in Figure 1), thus enhancing the electric communication between the grains. Electrophoretic deposition[2b] of the ternary component aggregates onto a nanostructured $SnO_2$ electrode allowed us to fabricate a desirable D–A SWNT film on the electrode (step 2 in Figure 1). To the best of our knowledge, the "wiring effect" of SWNTs between photoactive nanograins has never been investigated to date. Furthermore, this is the first

example of the ternary component system consisting of porphyrin, fullerene, and SWNTs, although the binary systems have been widely utilized for photo- and electronic devices.[4–6]

Novel porphyrin–$C_{60}$ linked dyad ($H_2$Por–$C_{60}$), porphyrin, and $C_{60}$ reference compounds ($H_2$Por-ref and $C_{60}$-ref) and highly soluble SWNTs (f-SWNT)[5,7] were synthesized according to reported procedures (Figure 2). Synthetic procedures

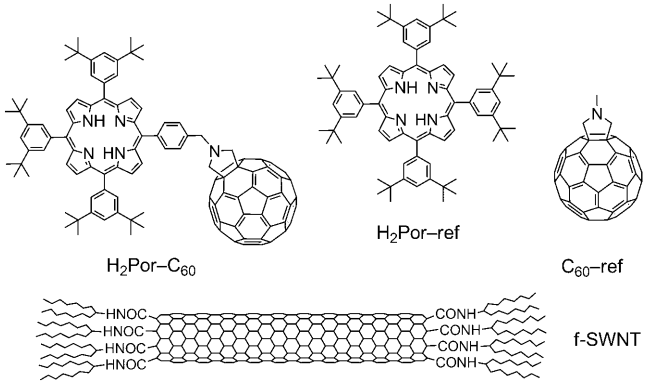


***Figure 2.*** Structures of $H_2$Por–$C_{60}$, $H_2$Por-ref, $C_{60}$-ref, and f-SWNT.

and photophysical and electrochemical properties are provided in the Supporting Information. Steady-state fluorescence measurements in *o*-dichlorobenzene (ODCB) indicate efficient photoinduced electron transfer (ET) from the porphyrin excited singlet state to $C_{60}$ in $H_2$Por–$C_{60}$. Emission from the porphyrin was strongly quenched compared to that from $H_2$Por-ref (Supporting Information, Figure S1). The occurrence of photoinduced ET was further confirmed by the femtosecond time-resolved transient absorption measurements (Supporting Information, Figure S2).

At first, self-assembling behavior of $H_2$Por–$C_{60}$ in an ODCB/acetonitrile mixture was investigated to better understand the nature of the more complex $H_2$Por–$C_{60}$ SWNT composite. The absorption spectrum of $H_2$Por–$C_{60}$ in ODCB exhibits a characteristic Soret band and Q bands (Supporting Information, Figure S3a). In the ODCB–acetonitrile mixture, the Soret and Q bands are broadened and red-shifted relative to those in ODCB (Supporting Information, Figure S3a). All of these changes are ascribed to the formation of nanograins of $H_2$Por–$C_{60}$ (denoted as $(H_2\text{Por–}C_{60})_m$),[2b] as described later. In contrast, the $H_2$Por-ref–$C_{60}$-ref composite (denoted as $(H_2\text{Por-ref} + C_{60}\text{-ref})_m$) does not show the broadening and shift of the Soret and Q bands (Supporting Information, Figure S3b). This indicates that $H_2$Por-ref molecules are not co-aggregating with $C_{60}$-ref efficiently to yield $(H_2\text{Por-ref} + C_{60}\text{-ref})_m$ during the self-assembly process.

In accord with the absorption behavior, the field-emission scanning electron microscopy (FE-SEM) measurement of $(H_2\text{Por–}C_{60})_m$ showed the presence of unique ellipsoid-shaped nanograins as large as 1.5–2.7 μm in the long axis and about 500 nm in the short axis (Figure 3a). In contrast, the FE-SEM image of $(H_2\text{Por-ref} + C_{60}\text{-ref})_m$ depicts irregular cubic structures with a small size of 50–100 nm (Figure 3b). The well-defined ellipsoid-shaped structure of $(H_2\text{Por–}C_{60})_m$ supports

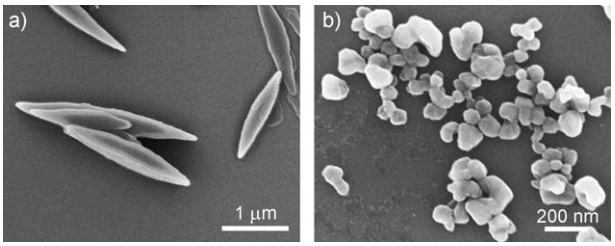


***Figure 3.*** FE-SEM images of a) $(H_2\text{Por–}C_{60})_m$ and b) $(H_2\text{Por-ref} + C_{60}\text{-ref})_m$. The samples were prepared by spin-coating the corresponding grain solutions ([porphyrin] = [$C_{60}$] = 0.16 mM) from an *o*-dichlorobenzene/acetonitrile mixture (2:5 v/v) onto a silicon wafer.

the proposal that $H_2$Por–$C_{60}$ molecules are well-organized in the nanograins. Furthermore, the X-ray diffraction (XRD) measurement of $(H_2\text{Por–}C_{60})_m$ revealed a weak diffraction peak at 11.6°, corresponding to an interplane distance of 7.3 Å (Supporting Information, Figure S4). According to the crystallographic study on the single crystal of $H_2$Por-ref,[8] this value is reasonably assigned as the inter-plane distance between the porphyrins in which one of eight *tert*-butyl groups of one porphyrin is fit into a one-sided hollow center of another porphyrin surrounded by the four *tert*-butyl groups. This results in a slipped stacked J-aggregate of the porphyrin moieties, consistent with the red shift of the Soret band. A similar J-like arrangement of porphyrin moieties has been implied in the rod-like aggregates of ionic porphyrin–$C_{60}$ dyads.[9] A plausible molecular structure of $(H_2\text{Por–}C_{60})_{10}$ optimized by the MM3 force field reveals the formation of slipped stacked porphyrin arrays with an interplane distance of 6–7 Å, where the $C_{60}$ moieties are arranged continuously along the one-dimensional (1D) porphyrin array (Supporting Information, Figure S5). The steady-state fluorescence of $(H_2\text{Por–}C_{60})_m$ shows strong quenching of the porphyrin fluorescence without exhibiting charge-transfer emission from the direct contact with the porphyrin and $C_{60}$.[2] All of these data suggest that the porphyrin moieties are stacked linearly and the $C_{60}$ moieties are closely located around the porphyrin alignment in the ellipsoid-shaped nanoaggregates.

Upon subjecting the resulting grain solution to a high electric (dc) field (200 V, 120 s), $(H_2\text{Por–}C_{60})_m$ and $(H_2\text{Por-ref} + C_{60}\text{-ref})_m$ were deposited onto nanostructured $SnO_2$ electrodes (denoted as FTO/$SnO_2$/$(H_2\text{Por–}C_{60})_m$ and FTO/$SnO_2$/$(H_2\text{Por-ref} + C_{60}\text{-ref})_m$).[2b] The absorption feature of the FTO/$SnO_2$/$(H_2\text{Por–}C_{60})_m$ electrode is largely similar to that in the corresponding ODCB/acetonitrile solutions (Supporting Information, Figure S6). On the other hand, the FTO/$SnO_2$/$(H_2\text{Por-ref} + C_{60}\text{-ref})_m$ electrode shows a structureless absorption feature resembling the $C_{60}$ absorption, supporting the proposal that little $H_2$Por-ref molecules are incorporated into the nanoaggregates as a result of weak π–π interactions between the porphyrin and $C_{60}$. The broad absorption of the fabricated films together with the high absorption in the visible region makes these films suitable for harvesting solar energy. The FE-SEM images of the FTO/$SnO_2$/$(H_2\text{Por–}C_{60})_m$ electrode (Figure 4a; Supporting Information, Figure S7a) display packing of the ellipsoid-shaped nanograins, which are almost identical to the spin-coated nanograins observed in

  

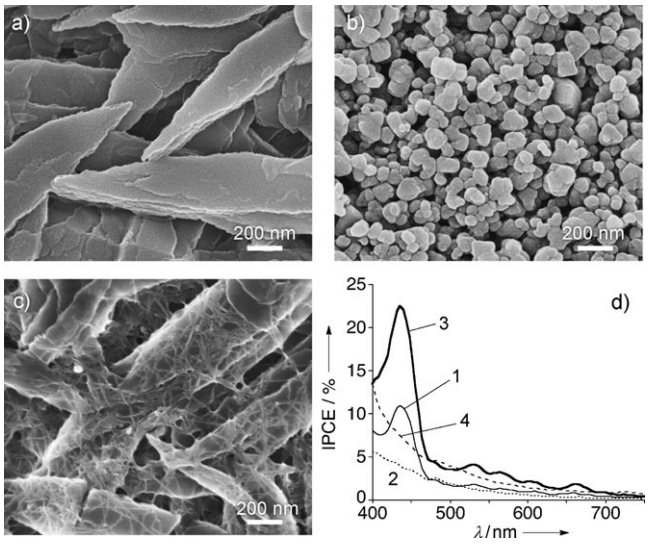


***Figure 4.*** FE-SEM images of a) FTO/$SnO_2$/$(H_2Por–C_{60})_m$, b) FTO/$SnO_2$/$(H_2Por\text{-ref}+C_{60}\text{-ref})_m$, and c) FTO/$SnO_2$/$(H_2Por–C_{60}+\text{f-SWNT})_m$ electrodes. d) Photocurrent action spectra of 1) FTO/$SnO_2$/$(H_2Por–C_{60})_m$, 2) FTO/$SnO_2$/$(H_2Por\text{-ref}+C_{60}\text{-ref})_m$, 3) FTO/$SnO_2$/$(H_2Por–C_{60}+\text{f-SWNT})_m$, and 4) FTO/$SnO_2$/$(H_2Por\text{-ref}+C_{60}\text{-ref}+\text{f-SWNT})_m$ devices. Applied potential: +0.17 V vs. SCE (see the Supporting Information, Figure S9). Electrolyte: 0.5 M LiI and 0.01 M $I_2$ in acetonitrile. IPCE = incident photon to current efficiency.

Figure 3a. This corroborates that fact that $(H_2Por–C_{60})_m$ was successfully deposited on the nanostructured $SnO_2$ electrode. In contrast, the FE-SEM image of the FTO/$SnO_2$/$(H_2Por\text{-ref}+C_{60}\text{-ref})_m$ electrode exhibits packing of the small cubic nanograins (Figure 4b; Supporting Information, Figure S7b).

To evaluate the charge-carrier mobility ($\mu$) of the FTO/$SnO_2$/$(H_2Por–C_{60})_m$ electrode, we measured the flash-photolysis time-resolved microwave conductivity (TRMC).[10] Upon exposure to a laser pulse with an excitation wavelength of 355 nm, the sample reveals a rise of the transient conductivity $\langle\phi\Sigma\mu\rangle$, in which $\phi$ is the quantum efficiency of charge separation (CS) and $\Sigma\mu$ is the sum of the mobilities of all the transient-charge carriers (Table 1; Supporting Information, Figure S8). The $\Sigma\mu$ value (0.30 $cm^2V^{-1}s^{-1}$) of the FTO/$SnO_2$/$(H_2Por–C_{60})_m$ electrode is very close to the highest value (2.0 $cm^2V^{-1}s^{-1}$) ever reported for analogous D–A arrays utilizing D–A linked systems,[2,10] demonstrating the superior carrier-transporting capability within the nanograins.

***Table 1:*** Microwave conductivity, quantum efficiency of CS, electron mobility, and maximal IPCE value.

| | $\phi\Sigma\mu$[a,b] [$cm^2V^{-1}s^{-1}$] | $\phi$[a,c] [%] | $\Sigma\mu$[a] [$cm^2V^{-1}s^{-1}$] | Maximal IPCE [%] |
|---|---|---|---|---|
| $(H_2Por–C_{60}+\text{f-SWNT})_m$ | $6.3\times10^{-3}$ | 0.2 | 3.1 | 22 |
| $(H_2Por–C_{60})_m$ | $1.8\times10^{-3}$ | 0.6 | 0.30 | 11 |

[a] $\phi$ = quantum efficiency of CS; $\Sigma\mu$ = sum of mobility of all the transient charge carriers. [b] Maximum value of the transient conductivity upon photoirradiation at 355 nm (photon density = $3.3\times10^{15}$ $cm^{-2}$). [c] Determined by a conventional DC-current integration technique with a photoexcitation at 355 nm.

To assess the macroscopic charge-transporting properties of the deposited films, we measured the wavelength-dependent incident photon to current efficiency (IPCE) spectra. Figure 4d depicts the photocurrent action spectrum of the FTO/$SnO_2$/$(H_2Por–C_{60})_m$ device under the three-electrode photoelectrohemical conditions.[2] The photocurrent action spectrum largely resembles the absorption spectrum of the deposited nanograins on the electrode (Supporting Information, Figure S6), implying the involvement of the porphyrin absorption for the photocurrent generation. In contrast, the photocurrent action spectrum of the FTO/$SnO_2$/$(H_2Por\text{-ref}+C_{60}\text{-ref})_m$ device shows structureless photocurrent response resembling the $C_{60}$ absorption owing to the limited incorporation of $H_2Por$-ref into the film. The maximum IPCE value (11% at 440 nm) of the FTO/$SnO_2$/$(H_2Por–C_{60})_m$ device is about three times as large as the corresponding value (4% at 440 nm) of the FTO/$SnO_2$/$(H_2Por\text{-ref}+C_{60}\text{-ref})_m$ device (Figure 4d). It should also be emphasized that the maximum IPCE value (11%) of the FTO/$SnO_2$/$(H_2Por–C_{60})_m$ device is the highest reported for analogous photoelectrochemical devices utilizing D–A linked systems under three-electrode conditions (4%).[2,10,11]

To examine the wiring effect of SWNTs on the charge-transport properties, we attempted to link the ellipsoid-shaped nanograins of $(H_2Por–C_{60})_m$ with f-SWNT to enhance the electric communication. Namely, initial self-assembly of $H_2Por–C_{60}$ with f-SWNT in the same mixed solvent leads to the formation of $H_2Por–C_{60}$–f-SWNT ternary composites (denoted as $(H_2Por–C_{60}+\text{f-SWNT})_m$) and subsequent electrophoretic deposition of the $(H_2Por–C_{60}+\text{f-SWNT})_m$ onto a FTO/$SnO_2$ electrode to give the deposited electrode (denoted as FTO/$SnO_2$/$(H_2Por–C_{60}+\text{f-SWNT})_m$).

The FE-SEM image of the FTO/$SnO_2$/$(H_2Por–C_{60}+\text{f-SWNT})_m$ electrode disclosed the expected morphology in which the ellipsoid-shaped nanoaggregates of $(H_2Por–C_{60})_m$ are connected with f-SWNT (Figure 4c; Supporting Information, Figure S7c). Atomic force microscopy (AFM) measurements also corroborate this cross-linked morphology (Supporting Information, Figure S10). It is noteworthy that the self-assembly processes allow f-SWNT to just bridge between the ellipsoid-shaped nanograins without affecting the intrinsic morphology of the $(H_2Por–C_{60})_m$. In accordance with the surface observation, the TRMC measurement on the FTO/$SnO_2$/$(H_2Por–C_{60}+\text{f-SWNT})_m$ electrode exhibited one order of magnitude higher transient conductivity than that of the FTO/$SnO_2$/$(H_2Por–C_{60})_m$ electrode (Supporting Information, Figure S8) to yield a $\Sigma\mu$ value of 3.1 $cm^2V^{-1}s^{-1}$, which is comparable to the value (3.2 $cm^2V^{-1}s^{-1}$)[5b,c] of the FTO/$SnO_2$/$(\text{f-SWNT})_m$ electrode without $H_2Por–C_{60}$ (Supporting Information, Figure S11). Note that the rise profile of the transient conductivity for the FTO/$SnO_2$/$(H_2Por–C_{60}+\text{f-SWNT})_m$ is different from that for FTO/$SnO_2$/$(\text{f-SWNT})_m$[5b,c] but close to that for the FTO/$SnO_2$/$(H_2Por–C_{60})_m$, reaching the conductivity maximum within 1 μs. Similarly, the photoresponse behavior of the TRMC signals implies that the large majority of the photocarriers in $(H_2Por–C_{60}+\text{f-SWNT})_m$ are generated by the excitation of $H_2Por–C_{60}$, that is, by CS between the porphyrin and $C_{60}$. Therefore, the improved $\Sigma\mu$ value of the FTO/$SnO_2$/$(H_2Por–C_{60}+\text{f-SWNT})_m$, which is

  

almost the same as that of the FTO/$SnO_2$/(f-SWNT)$_m$, can be interpreted by the occurrence of charge shift from the resulting $C_{60}^{\bullet-}$ to the f-SWNT, followed by bulk recombination of charge carriers during efficient electron transportation through the f-SWNT. In accordance with the f-SWNT wiring, the maximum IPCE value (22%) of the FTO/$SnO_2$/($H_2$Por–$C_{60}$ + f-SWNT)$_m$ device is twice as large as that of the FTO/$SnO_2$/($H_2$Por–$C_{60}$)$_m$ device (Figure 4d).[12] The FTO/$SnO_2$/(f-SWNT)$_m$ device showed an IPCE value of 1% at 440 nm (Supporting Information, Figure S12).[5b,c] These results unambiguously corroborate that electric communication between the D–A nanoaggregates is enhanced remarkably by the SWNT wiring.[13]

On the basis of the film structures, TRMC mobilities, and photoelectrochemical properties discussed above, as well as the previous studies on similar photoelectrochemical devices consisting of porphyrin–fullerene composites[14] and the fullerene–SWNT composites,[5] a mechanism of a photocurrent generation for the FTO/$SnO_2$/($H_2$Por–$C_{60}$ + f-SWNT)$_m$ device can be proposed (Supporting Information, Scheme S1). Photocurrent generation is initiated by the photoinduced ET from the porphyrin singlet excited state ($^1H_2$Por*/$H_2Por^{\bullet+}$ = −0.7 V vs. NHE) to the $C_{60}$ moiety ($C_{60}/C_{60}^{\bullet-}$ = −0.4 V vs. NHE), as shown by the time-resolved absorption measurements (Supporting Information, Figure S2) and the photoelectrochemical measurements (Figure 4d). The photoinduced ET occurs with a quantum efficiency near unity.[2] Then, the $C_{60}$ arrays mediate electrons to a conduction band (CB) of the f-SWNT ($c_1$ = −0.1 V vs. NHE).[5] ET from $C_{60}^{\bullet-}$ to f-SWNT is energetically favorable and demonstrated by results of the TRMC measurements[5b,c] (see above). Furthermore, intimate contact between f-SWNT and the nanograins of $H_2$Por–$C_{60}$ disclosed by the microscopic observation (Figure 4c; Supporting Information, Figure S10) promotes the electron mediation from $C_{60}^{\bullet-}$ to the f-SWNT. The superb electron mobility (3.2 $cm^2 V^{-1} s^{-1}$) of the f-SWNT facilitates the electron flow toward the $SnO_2$ electrode ($E_{CB} \approx 0$ V vs. NHE)[14] by electrically wiring the ellipsoid-shaped nanograins of $H_2$Por–$C_{60}$. On the other hand, the porphyrin arrays ($H_2Por/H_2Por^{\bullet+}$ = 1.2 V vs. NHE) shift holes until the oxidized porphyrin accepts electrons from the $I^-/I_3^-$ redox couple ($I^-/I_3^-$ = 0.5 V vs. NHE)[14] to regenerate the initial state. Finally, the electrons injected into the CB of the $SnO_2$ nanocrystallines are driven to the counter electrode by the external circuit to regenerate the $I_3^-/I^-$ redox couple.

In conclusion, we have developed a novel self-assembly method to build up well-organized D–A nanograins and simultaneous molecular wiring for efficient charge transport. The semiflexible short methylene linkage of $H_2$Por–$C_{60}$ without conventional extra self-assembling units allowed us to successfully form the unique ellipsoid-shaped nanograins in a good/poor solvent mixture by selectively enforcing porphyrin–porphyrin interactions and $C_{60}$–$C_{60}$ interactions rather than porphyrin–$C_{60}$ interactions. $H_2$Por–$C_{60}$ molecules in the nanograins were found to yield highly aligned D–A structures, making it possible to achieve efficient intracharge-transport within the nanograins. More importantly, the f-SWNT wiring between the D–A nanograins also rendered the intercharge-transport efficient, leading to the highest IPCE value (22%) reported for analogous photoelectrochemical devices utilizing D–A linked systems (4%).[2,10,11] We believe that the self-assembly of D–A linked molecules with molecular wires will be a highly promising method to achieve excellent device performances in organic photovoltaics and transistors.

Received: November 10, 2010
Published online: April 14, 2011

**Keywords:** charge transport · fullerenes · nanotubes · porphyrins · self-assembly

[1] a) H. Klauk, *Organic Electronics*, Wiley-VCH, Weinheim, **2006**; b) H. Sirringhaus, *Adv. Mater.* **2005**, *17*, 2411–2425; c) V. Coropceanu, J. Cornil, D. A. da Silva, Y. Olivier, R. Silbey, J. L. Bredas, *Chem. Rev.* **2007**, *107*, 926–952.
[2] a) H. Imahori, *Bull. Chem. Soc. Jpn.* **2007**, *80*, 621–636; b) H. Imahori, *J. Mater. Chem.* **2007**, *17*, 31–41.
[3] a) P. D. W. Boyd, C. A. Reed, *Acc. Chem. Res.* **2005**, *38*, 235–242; b) D. M. Guldi, N. Martin, *J. Mater. Chem.* **2002**, *12*, 1978–1992.
[4] a) D. M. Guldi, *Chem. Soc. Rev.* **2002**, *31*, 22–36; b) S. Fukuzumi, *Phys. Chem. Chem. Phys.* **2008**, *10*, 2283–2297; c) D. Gust, T. A. Moore, A. L. Moore, *Acc. Chem. Res.* **2001**, *34*, 40–48.
[5] a) T. Umeyama, N. Tezuka, M. Fujita, S. Hayashi, N. Kadota, Y. Matano, H. Imahori, *Chem. Eur. J.* **2008**, *14*, 4875–4885; b) T. Umeyama, N. Tezuka, S. Seki, Y. Matano, M. Nishi, K. Hirao, H. Lehtivuori, N. V. Tkachenko, H. Lemmetyinen, Y. Nakao, S. Sakaki, H. Imahori, *Adv. Mater.* **2010**, *22*, 1767–1770; c) N. Tezuka, T. Umeyama, S. Seki, Y. Matano, M. Nishi, K. Hirao, H. Imahori, *J. Phys. Chem. C* **2010**, *114*, 3235–3247.
[6] a) D. M. Guldi, G. M. A. Rahman, M. Prato, N. Jux, S. Qin, W. Ford, *Angew. Chem.* **2005**, *117*, 2051–2054; *Angew. Chem. Int. Ed.* **2005**, *44*, 2015–2018; b) T. Umeyama, M. Fujita, N. Tezuka, N. Kadota, Y. Matano, K. Yoshida, S. Isoda, H. Imahori, *J. Phys. Chem. C* **2007**, *111*, 11484–11493; c) F. D'Souza, A. S. D. Sandanayaka, O. Ito, *J. Phys. Chem. Lett.* **2010**, *1*, 2586–2593.
[7] The average length of the f-SWNT was estimated to be 380 nm by atomic force microscopy (AFM) measurements.
[8] K.-i. Sugiura, K. Iwasaki, K. Umishita, S. Hino, H. Ogata, S. Miyajima, Y. Sakata, *Chem. Lett.* **1999**, 841–842.
[9] V. Georgakilas, F. Pellarini, M. Prato, D. M. Guldi, M. Melle-Franco, F. Zerbetto, *Proc. Natl. Acad. Sci. USA* **2002**, *99*, 5075–5080.
[10] a) Y. Yamamoto, T. Fukushima, Y. Suna, N. Ishii, A. Saeki, S. Seki, S. Tagawa, M. Taniguchi, T. Kawai, T. Aida, *Science* **2006**, *314*, 1761–1764; b) Y. Yamamoto, G. Zhang, W. Jin, T. Fukushima, N. Ishii, A. Saeki, S. Seki, S. Tagawa, T. Minari, K. Tsukagoshi, T. Aida, *Proc. Natl. Acad. Sci. USA* **2009**, *106*, 21051–21056; c) F. Würthner, Z. Chen, F. J. M. Hoeben, P. Osswald, C.-C. You, P. Jonkheijm, J. Herrikhuyzen, A. P. H. J. Schenning, P. P. A. M. van der Schoot, E. W. Meijer, E. H. A. Beckers, S. C. J. Meskers, R. A. J. Janssen, *J. Am. Chem. Soc.* **2004**, *126*, 10611–10618; d) C. Röger, M. G. Müller, M. Lysetska, Y. Miloslavina, A. R. Holzwarth, F. Würthner, *J. Am. Chem. Soc.* **2006**, *128*, 6542–6543; e) W.-S. Li, Y. Yamamoto, T. Fukushima, A. Saeki, S. Seki, S. Tagawa, H. Masunaga, S. Sasaki, M. Takata, T. Aida, *J. Am. Chem. Soc.* **2008**, *130*, 8886–8887; f) R. Charvet, S. Acharya, J. P. Hill, M. Akada, M. Liao, S. Seki, Y. Honsho, A. Saeki, K. Ariga, *J. Am. Chem. Soc.* **2009**, *131*, 18030–18031; g) Y. Hizume, K. Tashiro, R. Charvet, Y. Yamamoto, A. Saeki, S. Seki, T. Aida, *J. Am. Chem. Soc.* **2010**, *132*, 6628–6629.
[11] a) P. V. Kamat, S. Barazzouk, S. Hotchandani, K. G. Thomas, *Chem. Eur. J.* **2000**, *6*, 3914–3921; b) H. Imahori, T. Hasobe, H.

  

Yamada, P. V. Kamat, S. Barazzouk, M. Fujitsuka, O. Ito, S. Fukuzumi, *Chem. Lett.* **2001**, 784 – 785.

[12] Film fabrication was carried out using $H_2$Por–$C_{60}$ (0.16 mM) with various concentrations of f-SWNT (from 6.3 to 19 mg $L^{-1}$). The subsequent photoelectrochemical measurements revealed that 13 mg $L^{-1}$ of f-SWNT yielded the highest IPCE values. Thus, the samples for all measurements were prepared with this concentration.

[13] Although the photocurrent response from the porphyrin is absent because very little $H_2$Por-ref is incorporated into the grains, the IPCE value of the FTO/$SnO_2$/($H_2$Por-ref + $C_{60}$-ref + f-SWNT)$_m$ device (see (4) in Figure 4 d) is also larger than that of the FTO/$SnO_2$/($H_2$Por-ref + $C_{60}$-ref)$_m$ device (see (2) in Figure 4 d) as a result of the wiring of the nanograins by f-SWNTs (Supporting Information, Figure S13).

[14] a) H. Imahori, M. Ueda, S. Kang, H. Hayashi, S. Hayashi, H. Kaji, S. Seki, A. Saeki, S. Tagawa, T. Umeyama, Y. Matano, K. Yoshida, S. Isoda, M. Shiro, N. V. Tkachenko, H. Lemmetyinen, *Chem. Eur. J.* **2007**, *13*, 10182 – 10193; b) P. V. Kamat, S. Barazzouk, K. G. Thomas, S. Hotchandani, *J. Phys. Chem. B* **2000**, *104*, 4014 – 4017.

  